Available online at www.sciencedirect.com

ScienceDirect

Procedia Engineering 149 (2016) 414 – 420

Procedia Engineering

www.elsevier.com/locate/procedia

International Conference on Manufacturing Engineering and Materials, ICMEM 2016, 6-10 June 2016, Nový Smokovec, Slovakia

Micro-structure in the joint friction plane in friction welding of dissimilar steels

Nada Ratković[a], Dušan Arsić[a,*], Vukić Lazić[a], Ružica R. Nikolić[a,b], Branislav Hadzima[b]

[a] *Faculty of Engineering University of Kragujevac, Sestre Janjić 6, 34000 Kragujevac, Serbia*
[b] *Research Center, University of Žilina, Univerzitna 8215/1, Žilina 010 26, Slovakia.*

Abstract

In the friction welding of dissimilar base metals occurs an uneven heating in the outside and inside zones of materials what causes appearance of various structures in the joint zone. Considering that the objective is achieving of the homogeneous welded joint, an imperative is to analyze the microstructure of the realized welded joint. By the microstructure analysis, one can establish the relationship between the friction welding parameters and the structure that appears in each of the joint's characteristic zones. In addition, it is possible to analyze the potential appearance of flaws during the welding process and to discover the causes for their appearance in order to prevent those in the future. This paper presents a review and analysis of microstructures of the characteristic joint zones in the friction plane of the two different steels, the high-speed steel and carbon steel for tempering. The experiment consisted of varying the friction welding parameters (friction pressure and friction time) and monitoring of micro structure in the joint zone and its immediate vicinity, both from the side of the tempering steel and the HS steel, as well as defining the present phases and compounds. The emphasis was set on analysis of the melting and the mixing zones and carbides created during the welding.

Peer-review under responsibility of the organizing committee of ICMEM 2016

Keywords: Friction welding, microstructure, friction plane, mixing zone, melting zone.

1. Introduction

The friction welding occupies an important place, whether it concerns the classical friction welding or the friction welding with mixing. The reason for that are the numerous advantages of the friction welding procedure, with respect to other welding procedures, primarily in regards with environmental protection and human health [1], while simultaneously one obtains the welded joints of the exceptional mechanical properties [2-5]. Analysis of mechanical properties, performed by Handa and Chawla in [2], has assumed studying of joining the austenitic and ferritic steels. That study consisted of the friction welding process parameter optimization, microstructure, mechanical characterization and fracture behavior. Their experimental results indicated that the axial pressure has a significant effect on the mechanical properties of the joint and that it is possible to increase the quality of the welded joint by selecting the optimum axial pressures. The same authors in paper [3] have shown the experimental results that indicate that the rotational speed and the axial pressure have a significant effect on the mechanical properties especially the torsional strength, impact strength and micro hardness. An analysis was conducted by Savić et al. in [4] of joining the high-speed steel HS 6-5-2C and the carbon steel C60, where an attempt was done to form a model of friction welding of the dissimilar materials, by monitoring the temperature cycles and variation of the microstructure during the welding process. Similar investigations were performed by authors in [5-7] where the results which are related to structural and chemical changes in the joint were presented, as well as to the influence of the welding parameters on the joint deformation – shortening and joint diameter. Those results have shown that one of the most important parameters is the welding time and that by its

* Corresponding author. Tel.:+381 64 276 39 81.
E-mail address dusan.arsic@fink.rs

Peer-review under responsibility of the organizing committee of ICMEM 2016
doi:10.1016/j.proeng.2016.06.686

Nomenclature

BM – Base metal;
HAZ – Heat affected zone;
WM – Weld metal;
L – Specimens' lengths;
d – Specimens' diameters;
n – Number of rpms;
p_c – Compacting pressure;
p_f – Friction pressure;
t – Thickness of the hard-faced layer;
t_f – Friction time;

extension the deformation of joints is increasing. The main conclusion is also that the joining of the two dissimilar steels can be realized, but that it is necessary to select the optimal welding parameters. That is also shown by some of the state-of-the-art researches [9-14], which were dealing with this problematics. Ma et al. [9] were investigating the friction welding of the two different steels – 1045 carbon steel and 304 stainless steel and performed a detailed analysis of microstructure and mechanical characteristics of the joint. Obtained results have shown that the weld interface can be clearly identified in the central zone, while the two metals interlock with each other by the mechanical mixing in the peripheral zone. On the carbon steel side, a thin pro-eutectoid ferrite layer was formed along the weld interface while on the stainless steel side the austenite grains were refined to a submicron scale. In addition, the existing δ-ferrite content in the stainless steel decreased from base metal towards the weld interface. It was also established that the severe plastic deformation plays a predominant role in rapid dissolution of the δ-ferrite, compared to the high temperature role. The carbide layer, consisting of CrC and Cr23C6 was formed at the weld interface because of elements' diffusion. Finally, it was also established that the carbide layer thickness significantly influences the tensile properties of the joint. On the other hand, Nathan et al. [10] were trying to investigate possibilities of application of the titanium alloys for manufacturing the tools for the friction stir welding (FSW), as well as the microstructural characteristics of the three tungsten based alloys FSW tools, viz. 90%W, 95%W and 99%W. The welded part was made of the high strength low alloy (HSLA) steel and plate thickness was 5 *mm*. The joint zones' micro structure was monitored by the SEM and the chemical compositions of the compounds by the EDS. In this investigation was found that the tool made of the 99% W doped with 1% La_2O_3 exhibited microstructural stability at elevated temperatures during the FSW process. Li et al. in [11] were investigating the joining of titanium and steel, where they were observing the influence of the rotational speed of parts on creation the non-metallic inclusions in the joint zone, as well as on the tensile strength and micro hardness of the welded samples. Results have shown that the morphology of the intermetallic compounds, mainly $TiFe_2$ and TiFe, created at the steel part, transformed from dispersive to laminar pattern, as the rotation speed increased from 400 to 1800 rpm, with a transition point of around 600 rpm. The highest tensile strength of 468 MPa, corresponding to the joint efficiency of 90%, was achieved at 600 rpm, where the valley value of equilibrium interfacial temperature was obtained. The similar problems, as considered in this paper, were investigated by Reilly et al. in [12], where the material flow during the FSW of aluminum and steel was monitored, as well as by Sarkara et al. in [13] and Kurt in [14] who were considering the material flow during the FSW of the two steels. They all monitored the influence of the material flow on the tool geometry, welding conditions (rotation speed, plunge depth, dwell time), and the surface state of the steel sheet (un-coated or galvanized). Based on the conducted research, it was possible to establish the consistent interpretation of the stick-slip conditions at the tool-work piece interface, addressing an elusive and long-standing issue in the modeling the heat generation in the friction stir processing. It was also determined in [13] that the flow zone size and ligament width increase with increasing tool penetration and that material flow during the FSW can be subdivided in two components, namely the rotational flow and the through thickness flow. A combination of the two components results in the spiraling motion of the plasticized material within the flow zone.

In this paper is presented an analysis of microstructure in different zones of the friction welded joint. Analysis involved the plane (zone) of friction in which the largest changes occur, due to introduced heat and the welding pressure. All the processes occurring in the friction plane were analyzed, especially the microstructure and appearance of carbides and carbide planes and their position in the joint during the process. The specific characteristics is also the fact that the joining by friction welding of the two steels is done, the high-speed steel (HS) and the carbon steel, which are very different with respect to their mechanical properties, chemical composition and structure.

2. General data on applied materials

The decisive role in materials selection had their applicability in industry. Bearing in mind the wide application of the high-speed steels in metal machining and their high price, it is economically more rational to manufacture the working part of the tool of the HS steel, while its holder is made of the carbon steel.

2.1. High-speed steel HS 6-5-2-5

The HS 6-5-2-5 (HS CrMO) is the molybdenum HS steel of the special type, which is alloyed with tungsten and cobalt, besides the molybdenum. The notations of this steel, in different standards, are DIN: S6–5-2–5, AISI M35, AFNOR: 6–5-2–5 and JUS: Č 9780. It is characterized by increased hardness and wear resistance at elevated temperatures, while the mechanical machinability remains satisfactory. It is used for manufacturing the highly strained tools, where the special requirements are for the high toughness, high cutting speeds, shavings of the large cross-sections, drilling of the stainless and thermos-resistant steels, etc. It is also applied for highly stressed milling cutters, profiling tools, spiral drills, threaders, taps and other cutting tools. The HS 6-5-2-5 steel is also convenient for casting, so it can be used for manufacturing the cast high-speed cutting tools according to special procedures.

The HS 6-5-2-5 steel's microstructure in the annealed conditions is ferritic substrate with carbide globules (Fig. 1.a). After the quenching, the micro constituents are martensite, austenite and carbides. The chemical composition of the HS 6-5-2-5 steel is given in Table 1.

2.2. Carbon steel for tempering C60

This steel belongs into a group of carbon steels with guaranteed chemical composition, aimed for tempering. The notations of this steel, in different standards, are DIN: C60, UK: En9, AISI: C1060, GOST: 60, AFNOR: SS55 and JUS: Č 1730.

The microstructure of the C60 steel is perlite-ferritic (Fig. 1.b) and it has the best hardenability of all the unalloyed steels. Generally, it is not convenient for joining by the fusion welding procedures. Improvement of machinability is achieved by normalization. The C60 steel possesses the high wear resistance, but low resistance to electrochemical and chemical corrosion (oxidation). It is sensitive to quenching in water. For eliminating the brittleness after tempering, it is necessary to cool the steel in the heated fluid (oil or water) from the tempering temperature, depending on dimensions; it is also prone to hardening in air. When this steel is forged in dies, it is allowed to exceed the prescribed temperatures for the maximum of 50 ºC, for the sake of better formability. The forged pieces have to be cooled slowly, and then immediately they should be annealed, namely they are subjected to normalization and tempering.

In the normalized or the tempered condition, this steel is used for manufacturing of parts in the automotive industry, bicycle industry, for parts in the general machine building, where the high straining or toughness are not required, like: shafts, bolts, even as the tool steel for the stone machining tools. The chemical composition of the C60 steel is given in Table 1.

Table 1. Chemical composition of the HS 6-5-2-5 and C60 steels

Alloying elements, %	C	Si	Mn	Cr	Mo	V	W	Co	P	S
HS 6-5-2-5	0.82	0.45	0.40	4	5	1.9	6.5	5.5	0.035	0.035
C60	0.63	0.194	0.82	-	-	-	-	-	0.045	0.045

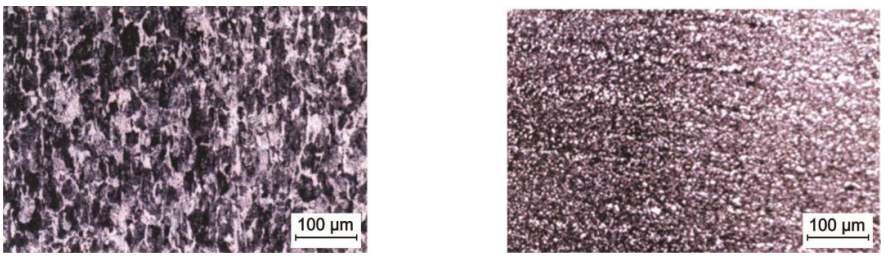

(a) (b)

Fig. 1. Characteristic microstructure of the HS 6-5-2-5 steel (a) and C60 steel in the annealed condition (b)

3. The welding procedure

The friction welding of the two cylindrical samples made of the HS 6-5-2-5 and C60 steels, shown in Fig. 2, was done. It was executed with the following parameters:

- number of rpms n = 2400 *rpms*,
- angular velocity 1.2 *m*/*s*,
- welding time t = (3÷18) *s*,
- friction pressure p_f = 70; 80; 90 *MPa*,
- compacting pressure p_c = (0÷210) *MPa*.

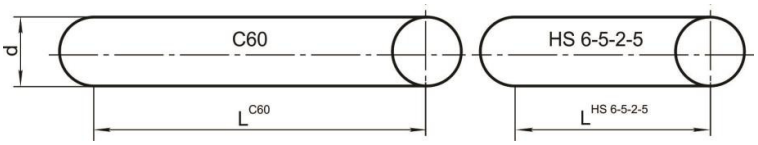

Fig. 2. Samples for friction welding

During the experiment, it was possible to select the friction pressure on the machine, the compacting pressure and the welding time in the rather wide range. What concerns the compacting time, the range is very narrow: shortening of the compacting time below 2.5 *s* causes worsening of the mechanical and other properties of the welded joint, while extending the compacting time above 4 *s* increases probability of appearance of cracks.

The friction pressure, during the third phase of the friction welding, when the temperature field is stabilized, should create conditions for extrusion of the undesired phases from the joint zone and prerequisites for the plastic deformation and forming of the metal bonds during the compacting phase. When operating with the excessively high pressures, the quantity of the released heat is increasing, however the quantity of the heat in the extruded metal is increasing, as well.

Optimal value of the compacting pressure (p_c) enables degree of deformation necessary for extrusion of the undesired phases from the joint, creation of the metal bonds of the frontal joint and creation of the joint without macroscopic flaws. The friction welding with the insufficiently high friction pressure (p_f) and too short friction time produces insufficient quantity of the released heat (low temperatures – narrow HAZ), thus for the unfavorable shape of the contact surfaces and creation of the undesired phases. It is necessary to introduce higher compacting pressure (p_c).

During the friction welding process, the sample of the C60 steel was moving towards the sample of the HS 6-5-2-5 steel, since it is easier deformable than the high-speed steel.

In order to evaluate the quality of the welded joints of those two steels, the experimental results were used, based on which one can estimate, among others, zones with the increased concentration of carbides, Fig. 3.

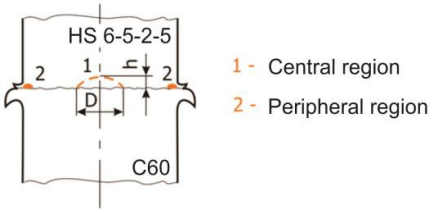

Fig 3. The usual position and shape of the area with the increased concentration of carbides in the high-speed steel (longitudinal section): *D* – central area diameter, *h* – penetration depth.

4. Microstructure in the area of the friction plane

An uneven plastic deformation occurs during the friction welding of dissimilar base metals. For instance, when the high-speed steel is welded with the tempering steel, at angular velocities of 500 to 2000 *rpm*s, the high-speed steel piece becomes buckled; the radius of the curvature of the deflected portion depends on the friction process on the confronted surfaces. Due to the later action of the axial pressure that buckled (deflected) zone becomes flatten, more prominently in the zones with the higher friction velocities. In the zones of sharp and deep jamming of the high-speed steel into the tempering steel appears the danger of areas with lack of penetration [8].

In addition, it was established that during the friction phase, the layer of the high-speed steel, approximately 50 μm thick, becomes hard-faced onto the tempering steel surface [8], thus the friction pair is high-speed steel for both pieces. Carbides on the frontal surface of the high-speed steel are polishing the contact surface, especially during the friction phase, then in the compacting phase due to additional plastic deformation the partial or complete destruction of carbide zones occurs. Those zones usually appear in the central portion of the bar, with diameter 0.5 to 3 *mm*. The metal structure in the carbide zones consists of martensite with 0.5 to 0.55 % of the residual austenite with more than 40 % of the dispersed carbides. The carbides' dimensions are up to 0.02 μm and mainly those are the MeS types of carbide (V, Mo, W). In this temperature range (in the friction phase) the ratio of the MeS carbides to $Cr_{23}C_6$ increase to value 1.1.

Based on the numerous investigations and monitoring of phenomena occurring during the friction phase, the conclusion was drawn that some experimental investigations are necessary as well, in order to explain certain phenomena and to establish the relationship between the friction welding parameters and the microstructural changes. Those experiments enabled categorization of the welded joints flaws and then ranking of the influential factors causing those flaws, primarily the friction time.

The experiments assumed monitoring the shape, size, distribution and microstructure of the HS 6-5-2-5 layer, which was spontaneously hard-faced onto the C60 steel surface, during the friction phase. The shape of the joint line was also monitored. Then, an analysis was conducted with respect to the shape, distribution and share of the carbide phase in the HS 6-5-2-5 steel, the

shape of the mixing zone of the both BM, description of the noticed cracks and evaluation of appearance and share of the residual austenite in the HS 6-5-2-5 steel.

The assumption that actually the hard-facing occurred, and not just breaking of the micro-bonds during the friction welding process, was confirmed by existence of the hard-faced layer of the HS 6-5-2-5 steel onto the C60 steel surface, which is in the friction phase being extruded into the wreath. To verify this statement, the samples were welded, subjected only to the friction phase, while the compacting was omitted. Then, the samples were separated and additional corresponding tests were performed. In Fig. 4 is given the schematic presentation of the shape and position of the HS 6-5-2-5 steel layer hard-faced onto the C60 steel.

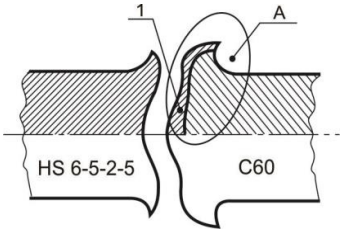

Fig. 4. The HS 6-5-2-5 (1) layer hard faced onto the C60 steel in the friction phase (region A)

Results show that the change of the friction time imposes almost no influence on the thickness of the hard-faced layers in the peripheral zones of the sample. However, after 14 *s*, somewhat thinner hard-faced layers were obtained. The thickness of the hard-faced layer was within limits 0.05 to 0.2 *mm*. In Fig. 5 is shown the shape of the hard-faced layer of the HS 6-5-2-5 steel, for different friction times, as well as the microstructure on the peripheral portion of the sample (a), in the zone of the extruded material (wreath) (b) and in the central zone of the sample in the mixing zone of both BM (c).

It is assumed that the smaller particles of the HS 6-5-2-5 steel are being transferred onto the C60 steel in the peripheral zones of the sample, during the phase I and at the beginning of the phase II of friction, which is not the case in the central zone. The thickness of the hard-faced layer extruded into the wreath amounted to 0.02 to 0.3 *mm*, while in the time interval between 11 *s* and 13 *s* the hard-faced layer of thickness 0.02 to 0.06 *mm* was obtained.

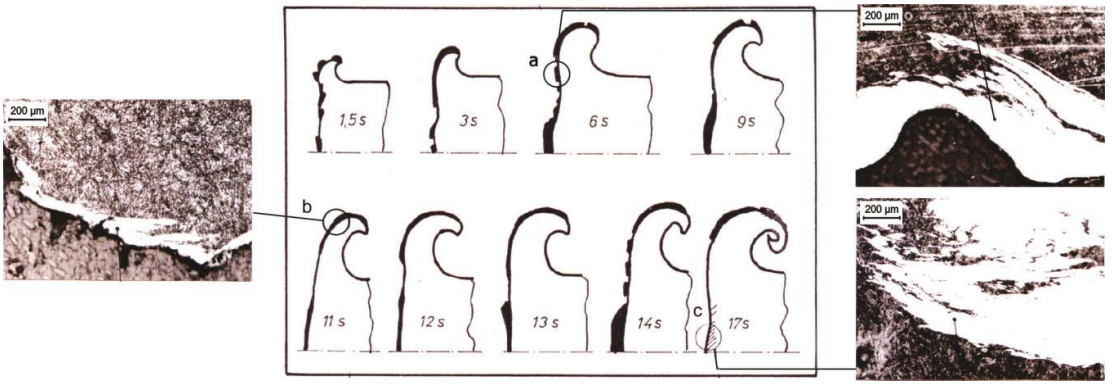

Fig. 5. Schematic presentation of the HS 6-5-2-5 steel layer hard-faced onto the frontal surface of the C60 steel and microstructure of welded joint zones: (a) zone between the central and peripheral portions of the sample (friction time 6 *s*); zone outside the friction plane (friction time 11 *s*); (c) zone of the two base metals mixing (friction time 17 *s*);

Thickness of the HS 6-5-2-5 steel layer hard-faced onto the C60 steel in the central portion of the sample varies with the friction time. For the friction time of 6 *s,* this layer reaches the maximal thickness (0.5 *mm*), and then all the way to 12 *s* the thickness decreases. For the friction time between 13 and 15 *s* the thickness increases again (even up to 0.8 *mm*), while the further extension of the friction time would cause decrease of the thickness below 0.3 *mm*. The measured value of the hard-faced layer thickness of 0.8 *mm* represents the maximal possible value for this pair of the base metals.

The microstructure of the HS 6-5-2-5 steel layer hard-faced onto the C60 steel during the friction welding process for the friction pressure $p_f = 80$ *MPa* and friction time $t_f = 12$ *s* and no compacting pressure, $p_c = 0$, is shown in Fig. 6.

The microstructures in different zones on the C60 carbon steel side (Fig. 6) at the weld interface varies along the radial direction. In the central zone the weld interface could be identified but due to the severe plastic flow of material C60 and HS 6-5-2-5 are mixed and interlocked. In addition, a thin pro-eutectoid ferrite layer was formed close to the C60 carbon steel. Since the temperature during the process is sufficiently high to austenitizing the material during the short cooling time, coarse perlite grains and less ferrite precipitating at perlite grain boundaries can occur [9]. Besides that, the Widmanstätten structure was

possible to identify within the structure, as well. Also in the zones where somewhat lower temperature was reached and the complete austenitizing did not occur, the content of ferrite was slightly higher, while the share of the brittle phases was lower.

Results also have shown that during the friction welding, the carbide plane is formed (position 1 in Fig. 6), in the friction plane region, at the frontal surface of the C60 element, whose front towards the friction plane is completely even (smooth), while on the opposite side the carbides are inserted into C60. The microstructure of HS 6-5-2-5 was mainly martensitic, with presence of the complex carbides, while the microstructure of C60 was mainly martensite-bainite one. The friction surface, in some places, can have wavy pattern what implies that during the friction phase the material had turbulent motion to a certain degree, Fig. 7.

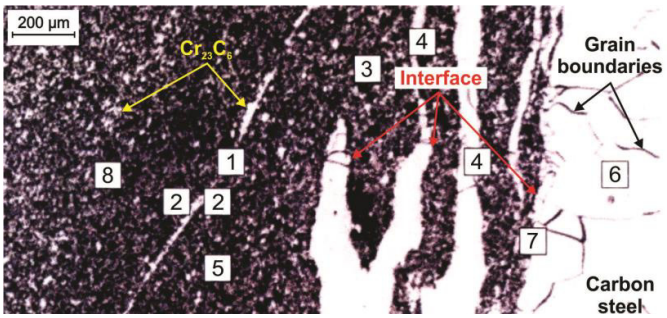

Fig. 6. Microstructure in the HS 6-5-2-5 steel layer hard-faced onto the C60 steel: 1 – carbide plane formed next to the friction plane; 2 – viscous layer; 3 – the hard-faced layer; 4 – the HS 6-5-2-5 and C60 mixing zone; 5 – zone of dynamic recrystallization; 6 – BM (C60); 7 – the joint line; 8 – HAZ in HS 6-5-2-5.

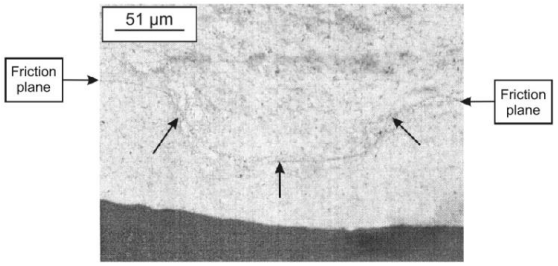

Fig. 7. Microstructure of the HS 6-5-2-5 steel in the friction plane region (welding without the additional pressure, p_f = 80 MPa, t_f = 12 *s*).

During the friction welding, the tearing of the HS 6-5-2-5 particles occurs and their transfer onto the C60, due to uneven deformation in the cross-section, relatively high friction velocity (n = 2400 *rpm*) and relatively high pressures (p_f = 80 *MPa*). Transfer of larger particles occurs in the central region. The particles within the hard-faced layer, as well as from the rest of the HS 6-5-2-5, are moving and carrying the particles of the carbide phase. Their share at the beginning of the friction process is more than 20 %. That share is decreasing with the progress of the friction phase due to dissolving in the austenite (the solid solution) and retaining at the frontal part of the rotating piece, and to a somewhat smaller extent due to extruding out of the friction plane. At the end, after cooling (solidification and transformation in the solid state), the viscous layer of a certain thickness can be seen on both sides of the friction plane. The structure of this layer is characterized by somewhat larger crystal grains and lower content of the carbide phases, with respect to the adjoining layers.

The friction plane in the central area of the sample (around the axis) divides the viscous layer into two parts. The carbide layer is created next to the friction plane on the HS 6-5-2-5 side. The viscous layer in the central part of the sample was formed generally parallel to the joint line, while in the regions of the sample close to the perimeter it is inclined at a certain angle, Fig. 8. This leads to the conclusion that in the friction plane, besides the dominant laminar and rotational flow, some other mechanism of the viscous metal mass flow occurred within the viscous layer.

At the end, it should be mentioned that hardness was measured throughout the welded joint and that the value in the HAZ of the HS 6-5-2-5 steel was around 350 HV, while it was decreasing with the distance from the joint line. The characteristics structure was martensite, residual austenite and carbides. The C60 steel hardness did not exceed 185 HV.

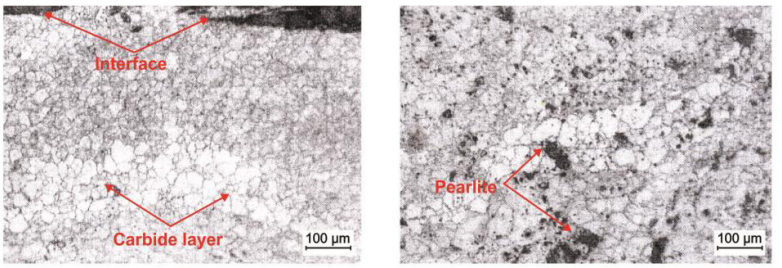

Fig 8. Microstructure of the viscous layer in the cross-section of the friction welded joint of the HS 6-5-2-5 and C60 steels (p_f = 80 MPa, t_f = 15 s, no compacting): (a) sample's central region; (b) sample's peripheral region.

5. Conclusions

Based on the presented results, the following conclusions can be drawn:

- During the friction welding, in the friction zone of materials, besides tearing of the micro-bonds also occurs hard-facing of the HS 6-5-2-5 steel onto the C60 steel. That hard-faced layer is partially extruded into the wreath while the part of it remains in the central portion of the sample;
- The friction time does not influence significantly the thickness of the welded joint. However, it influences the thickness of the hard-faced layer. The thinner hard-faced layer is obtained with the friction time increase: after t_f = 6 *s* the thickness is s = 0.5 *mm*; after t_f = 11 *s* the thickness is s = 0.5 *mm*. The maximal thickness is achieved at t_f = 11 *s* and it is s_{max} = 0.8 *mm*; however it is only temporary, since at time t_f = 16 *s* and it decreases to s = 0.3 *mm*.
- In the friction plane on the side of the HS 6-5-2-5 steel appears the carbide layer with maximum share of carbides of 20 %, but it decreases with increase of the friction time.

Acknowledgements

This research was partially financially supported by European regional development fund and Slovak state budget by the project "Research Centre of the University of Žilina" - ITMS 26220220183 and by the Ministry of Education, Science and Technological Development of Republic of Serbia through grants: ON174004, TR32036, TR35024 and TR33015.

REFERENCES

[1] Veljić D, Sedmak A, Rakin M, Radović N, Popović N, Dascau H, Bajić N. Advantages of friction stir welding over welding with respect to health and environmental protection and work safety. Structural Integrity and Life 2015;15(2):111-116.
[2] Handa A, Chawla V. Mechanical characterization of friction welded dissimilar steels at 1000 rpm. Materials Engineering 2013;20(3):102-111.
[3] Handa A, Chawla V. Influence of process parameters on torsional strength, impact toughness and hardness of dissimilar AISI 304 and AISI 1021 friction welded steels. Materials Engineering 2014;21(3):94-103.
[4] Savić B, Marković S, Ćirić R. Physical model of the friction welded joint of different types of steel. FME Transactions 2008;36(2):93-97.
[5] Ratković N, Nikolić R, Samardžić I. Structural, chemical and deformation changes in friction welded joint of dissimilar steels. Metallurgy 2014;53(4):513-516.
[6] Ratković N, Sedmak A, Jovanović M, Lazić V, Nikolić R, Krstić B. Physical and metallurgical changes during the friction welding of the high-speed steel and the tempering steel. Technical Gazette 2009;16(3):27-31.
[7] Ratković N, Arsić D, Lazić V, Nikolić R, Hadzima B. The contact and compacting pressures influences on the quality of the friction welded joint. Materials Engineering 2016;23:(in press)
[8] Ratković N, Modelling of the machine parts of various forms of the welding process. Doctoral dissertation. Faculty of Mechanical Engineering. Kragujevac, Serbia; 2009.
[9] Ma H, Qin G, Geng P, Li F, Fu B, Meng X, Microstructure characterization and properties of carbon steel to stainless steel dissimilar metal joint made by friction welding, Materials and Design 2015;86:587-597.
[10] Nathan S.R, Balasubramanian V, Malarvizhi S, Rao A.G, An investigation on metallurgical characteristics of tungsten based tool materials used in friction stir welding of naval grade high strength low alloy steels, International Journal of Refractory Metals and Hard Materials 2016;56:18-26.
[11] Li X, Li J, Liao Z, Jin F, Zhang F, Xiong J, Microstructure evolution and mechanical properties of rotary friction welded TC4/SUS321 joints at various rotation speeds, Materials and Design 2016;99:26-36.
[12] Reilly A, Shercliff H, Chenb Y, Prangnell P, Modelling and visualisation of material flow in friction stir spot welding, Journal of Materials Processing Technology 2015;225:473-484.
[13] Sarkara R, Pala T.K., Shome M., Material flow and intermixing during friction stir spot welding of steel, Journal of Materials Processing Technology 2016;227 96-109.
[14] B. Kurt, The interface morphology of diffusion bonded dissimilar stainless steel and medium carbon steel couples, Journal of Materials Processing Technology 2007;190:138-141.